CALIBRATION AND EXPERIMENTATION OF DISCRETE META-SIMULATION PARAMETERS OF ASTRAGALUS MEMBRANACEUS
/
黄芪离散元仿真参数的标定与试验

Xiangyu GAO [1,2], Xuejie MA[1], Xiangdong LIN*[1], Qianqian SUN*[1], Zhanfeng HOU *[1,3], Xiaoming ZHANG*[4]
[1] College of Mechanical and Electrical Engineering, Inner Mongolia Agricultural University, Inner Mongolia, Hohhot/ China
[2] Inner Mongolia First Machinery Group Corporation, Baotou/ China
[3] Inner Mongolia Engineering Research Center of Intelligent equipment for the entire process of forage and feed production, Inner Mongolia, Hohhot/ China
[4] Hohhot Agriculture and Animal Husbandry Technology Promotion Center, Hohhot, Inner Mongolia/ China
Corresponding auther: Xiangdong Lin, Qianqian Sun, Zhanfeng Hou, Xiaoming Zhang
Tel: +8613171058429; E-mail: njau-hzf@163.com
DOI: https://doi.org/10.35633/inmateh-73-71

Keywords: *astragalus membranaceus, angle of repose, relative error, parameter calibration, EDEM*

ABSTRACT
This study is based on the discrete element method to calibrate the physical parameters of astragalus membranaceus. Plackett Burman test, steepest climb test, and Box Behnken test were used to screen for significant influencing factors and optimal levels, and a quadratic regression model was obtained for the relative error between the simulated and physical experiment resting angles. The results showed that the relative error between the simulated and physical test angles of repose was only 0.392%, which can provide a theoretical basis for the discrete element simulation test of the working process of the astragalus membranaceus picking machine.

摘要
本研究基于离散元法对黄芪物性参数进行标定，采用 Plackett-Burman 试验，最陡爬坡试验，Box-Behnken 试验筛选出显著影响因素及最优水平，得到仿真试验休止角与物理试验休止角相对误差的二次回归模型。结果表明：仿真试验休止角与物理试验休止角相对误差仅为 0.392%，可为黄芪捡拾机工作过程的离散元仿真试验提供理论依据。

INTRODUCTION
Astragalus, a traditional Chinese herbal medicine, has been used medicinally for more than 2000 years and is one of the Chinese herbs with a large clinical dosage in traditional Chinese medicine. Astragalus is 50-100 cm long, with a thicker cylindrical rhizome part, light brownish-yellow or greyish-white in colour, and has a bean flavour when consumed (*Kang et al., 2016; Wu et al., 2004; Huang et al., 2023; Shen et al., 2023*).

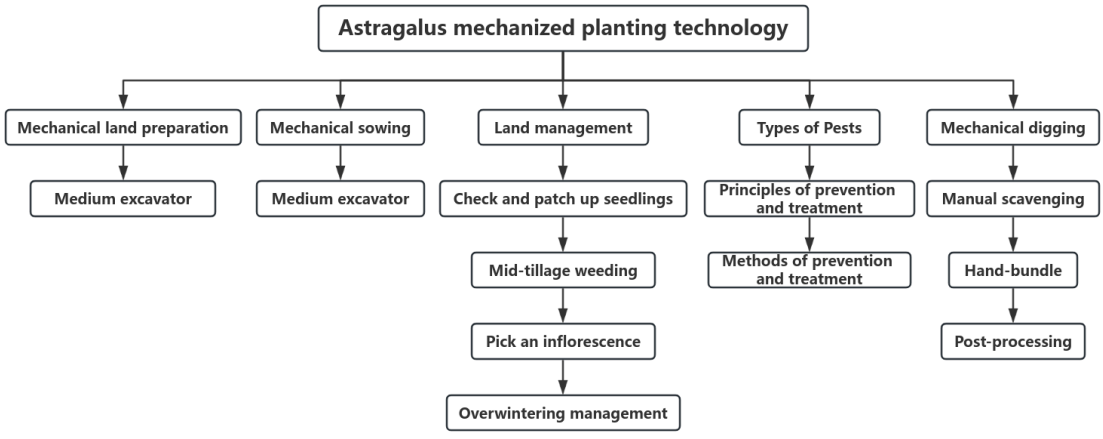

Fig. 1 - Mechanized planting of astragalus industry

As shown in Figure 1, some planting scale astragalus industry has basically realized the mechanized planting of astragalus, but in the harvesting stage of astragalus, due to the depth of astragalus planting up to 400 mm below ground, it adopts a segmented harvesting method, which is firstly dug by the astragalus harvester for astragalus, and then hiring the farmers to carry out the manual gleaning operation (*Jiang et al., 2013; Zhang et al., 2006; Li et al., 2015*). Artificial gleaning operation efficiency is low and the cost is high, so there is a need to develop and design a kind of astragalus gleaning machine applied to the astragalus industry, and to use the astragalus gleaning machine instead of the traditional manual gleaning operation, so as to reduce the amount of manual work, save cost, improve the efficiency of the astragalus gleaning operation, and achieve the mechanization of the astragalus industry (*Cui et al., 2014; Zhao et al., 2017*).

MATERIALS AND METHODS

Astragalus picker discrete element simulation model shown in Figure 2, astragalus picker in the working process, due to the operation of the picker components, there is a collision between the astragalus and the picker components, astragalus force including astragalus - astragalus, astragalus – steel; the force relationship is very complex, the magnitude of the astragalus collision force suffered by the astragalus will have a direct effect on the extent of damage to the astragalus epidermal skin, was shown in the use of the discrete element method of the astragalus picker work process. Numerical simulation of the working process of the astragalus picker using the discrete element method is conducive to revealing the working principle of the astragalus picker and further calibrating and optimizing the working parameters of the astragalus picker.

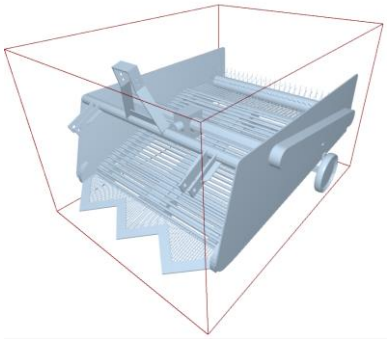

Fig. 2 - Discrete element modelling of astragalus picker

Before carrying out the research on the factors affecting the performance of the astragalus picker, since no researcher has calibrated and benchmarked the discrete element simulation parameters of the astragalus, it is necessary to calibrate the astragalus parameters to ensure the accuracy of the working parameter settings of the environment of the discrete element simulation software during the subsequent simulation experiments (*Chen et al., 2018*).

Determination of basic physical property parameters

First, the basic physical parameters of astragalus which are easy to measure were determined. Digital vernier callipers were used to determine the external dimensions of astragalus, and the parameters of the external dimensions of astragalus are shown in Table 1.

Table 1

External dimension parameters of astragalus

Projects/Unit	Target value
Astragalus length (mm)	300~690
Reed head diameter (mm)	11~21
Center Diameter (mm)	10~18
Root Diameter (mm)	10~17

Table 2

Basic physical parameters of astragalus segment

Projects/Unit	Target value
Overall dimensions (mm)	25.7±6.3×11.3±1.3
Mass (g)	9.95±2.15
Densities (kg·m^{-3})	0.912±0.159

Due to the large size of the astragalus, the error in measuring the physical parameters was large, so the astragalus was cut into astragalus segments of different sizes for the determination of astragalus. The weight of the astragalus segments was measured using an electronic balance, the length and diameter of the segments were measured using vernier callipers (L×D), and the density of the astragalus was measured using a measuring cylinder. The mean values of the measurement results are shown in Table 2.

As shown in Figure 3, the pressure deformation test of astragalus was carried out by using the texture instrument. Before the test started, the astragalus segment was placed horizontally on the test platform, the working parameters of the texture instrument were set, and loading was carried out at a speed of 5 mm/s in the thickness direction of astragalus, and when the deformation of the astragalus reached 30%, the loading was stopped and the press returned to the initial position. The thickness and width of the astragalus segments were measured before the test. The thickness and width of the astragalus segments were measured again after the press finished loading the astragalus in the thickness direction and returned to the initial position. Using equation (1), the Poisson's ratio of the astragalus was calculated according to the deformation of the astragalus segments in the width and thickness directions before and after loading.

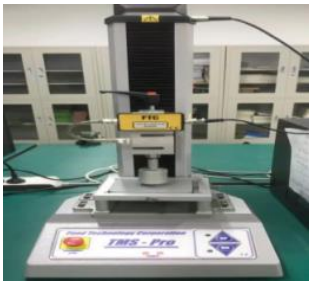

Fig. 3 - Texture analyzer

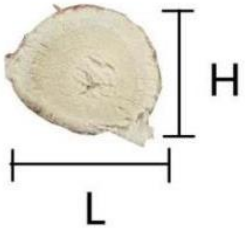

Fig. 4 - Diagram of astragalus membranaceus

$$\nu = \frac{|\varepsilon'|}{|\varepsilon|} = \frac{L_1 - L_2}{H_2 - H_1} \quad (1)$$

ν - the Poisson's ratio;
ε' - the transverse deformation;
ε - the longitudinal deformation;
L_1 - the width of astragalus before loading;
L_2 - the width after loading of astragalus;
H_2 - represents the thickness after loading of astragalus;
H_1 - represents the thickness of astragalus before loading.

Determination of exposure parameters

The contact parameters required when applying the discrete element method to study the law of motion of astragalus and the working principle of astragalus picker are static friction, rolling friction, and collision recovery coefficient between astragalus and astragalus; static friction, rolling friction, and collision recovery coefficient between astragalus and steel; and collision recovery coefficient between astragalus and rubber. In order to improve the accuracy of the contact parameters, a combination of physical tests and simulation tests will be used to determine the required contact parameters through physical tests, and the range of the required parameters to carry out the discrete element simulation tests will be determined by physical tests as a reference.

The physical test of the contact parameters was conducted using the cut and treated astragalus segments with a density of 0.912 g/cm^3, and the material in contact with the astragalus was steel with a density of 7,850 kg/m^3, a Poisson's ratio of 0.3, a shear modulus of 80 GPa, and a modulus of elasticity of 2.06×10^5 MPa.

Determination of crash recovery coefficient

The collision recovery coefficient indicates the ability of the object under test to recover its original state after a collision, and is defined as the ratio between the velocity of the object under test after collision and separation and the velocity before the collision. In this paper, free-fall physical tests were used to determine the collision recovery coefficients between astragalus and astragalus, astragalus and steel, and astragalus and rubber, and the test setups are shown in Fig. 5.

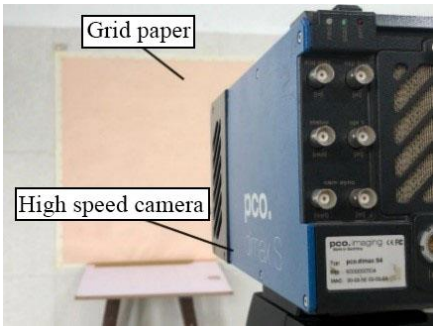

Fig. 5 - High speed camera

A high-speed camera was placed directly in front of the test bench and the tripod was adjusted to keep it horizontal, and the distance between the high-speed camera and the test bench was 780 mm. In order to facilitate the TEMA high-speed camera analysis software to capture the movement process of the astragalus, a piece of grid paper was arranged at the back of the test bench, so that the rebound height of the astragalus could be accurately observed.

Assuming that the astragalus is subjected only to gravity during its fall, the normal velocity of the astragalus before the collision is obtained from the kinetic energy theorem:

$$v_1 = \sqrt{2gh_1} \tag{2}$$

Normal velocity after collision separation:

$$v_2 = \sqrt{2gh_2} \tag{3}$$

From the definition of collision recovery coefficient, the collision recovery coefficient is obtained as:

$$e = \frac{|v_2|}{|v_1|} = \sqrt{\frac{h_2}{h_1}} \tag{4}$$

v_1 - the speed of astragalus before collision;

v_2 - the velocity of astragalus after collision;

h_1 - represents the astragalus fixed drop height;

h_2 - represents the astragalus rebound height after collision (*Dai et al., 2021*).

In this physical test, the height of the falling astragalus was fixed at 400 mm, and different astragals were selected to repeat the test, and the collision recovery coefficients between astragalus and rubber were obtained as 0.3142±0.013; between astragalus and astragalus as 0.3±0.1; and between astragalus and steel as 0.35±0.05.

Determination of static and rolling friction coefficients

The coefficient of static friction and the rolling friction coefficient between astragalus and astragalus, astragalus and steel were measured using CNY-1 type inclinometer (Figure 6).

Fig. 6 - CNY-1 inclinometer

In order to accurately measure the coefficient of static friction and coefficient of rolling friction between astragalus, before the test started, the astragalus and the test plane of the inclinometer were glued together by using transparent double-sided adhesive tape, and then the astragalus segments were placed along the length of the test plane of the inclinometer on the astragalus determination plane.

The test was conducted by slowly rotating the inclinometer test plane counterclockwise, immediately stopping rotating when the astragalus segment slides on the astragalus determination plane, recording the angle indicated by the inclinometer pointer at this time, through which the static friction coefficient and rolling friction coefficient between the astragalus can be calculated (*Zhang et al., 2018*). When determining the coefficient of static friction and coefficient of rolling friction between astragalus and steel plate, it is only necessary to change the test plane to steel plate.

Through 20 test trials and taking the average value, the average values of static friction coefficient and rolling friction coefficient between astragalus and astragalus were obtained as 0.65±0.03 and 0.53±0.03 respectively, and the average values of static friction coefficient and rolling friction coefficient between astragalus and steel plate were obtained as 0.2±0.1, and 0.15±0.05 respectively.

Determination of angle of repose of astragalus

According to the review of relevant literature, the test of measuring the angle of repose of astragalus segments was carried out by using the pumping plate method, the randomly selected astragalus was loaded into a closed cardboard box, the baffle plate on one side of the cardboard box was pumped vertically upward, so that the astragalus was free to slide down, and when the astragalus in the box was free to slide down and come to a standstill on the substrate, the astragalus heap was photographed with a camera, and a front-view picture of the heap of the astragalus was obtained, and the grayscale and binary processing was carried out for the picture by applying the software of Matlab. The image digitizing tool in Origin2018 software was applied to extract the boundary curve for fitting treatment, and the average value of the rest angle was obtained as 35.79° (Figure 7).

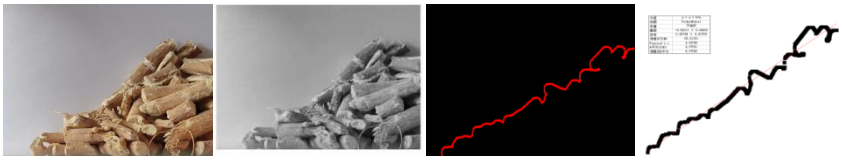

Fig. 7 - Image processing of astragalus accumulation

RESULTS

Parameter calibration for discrete meta-simulation of astragalus

According to Table 1 - astragalus external dimensions parameter list, the astragalus was modelled in Solidworks software, and the modelling file was imported into EDEM2018 software, and 121 basic spheres with a radius of 8 mm (the radius of the basic sphere is R_{min}) in the EDEM software library were used to fill out the simulation model of astragalus, which is shown in Figure 8.

Fig. 8 - Whole plant model of astragalus

Fig. 9 - Segmental model of astragalus membranaceus

In the physical parameter calibration simulation test of astragalus, the astragalus segments after the cutting treatment were used, and according to Table 2, the average diameter of astragalus segments was obtained as 11 mm, and the average length was obtained as 25 mm, and the shape of astragalus segments was approximate to a cylinder, so the simulation model of astragalus segments was populated by using five basic spheres with a radius of 5.5 mm in the library of the EMEM2018 software as shown in Figure 9.

The modelling of the simulated angle of repose determination apparatus for astragalus was based on the actual angle of repose determination apparatus. Considering the feasibility of the experiment and the high efficiency of the software operation, discrete element models of astragalus segments with different sizes were used in the simulation. The total simulation time was set to 10 s, the time step was 7.43678×10^{-5} s, and the grid size was $3\times R_{min}$. The working parameters of EDEM software were set as shown in Figure10.

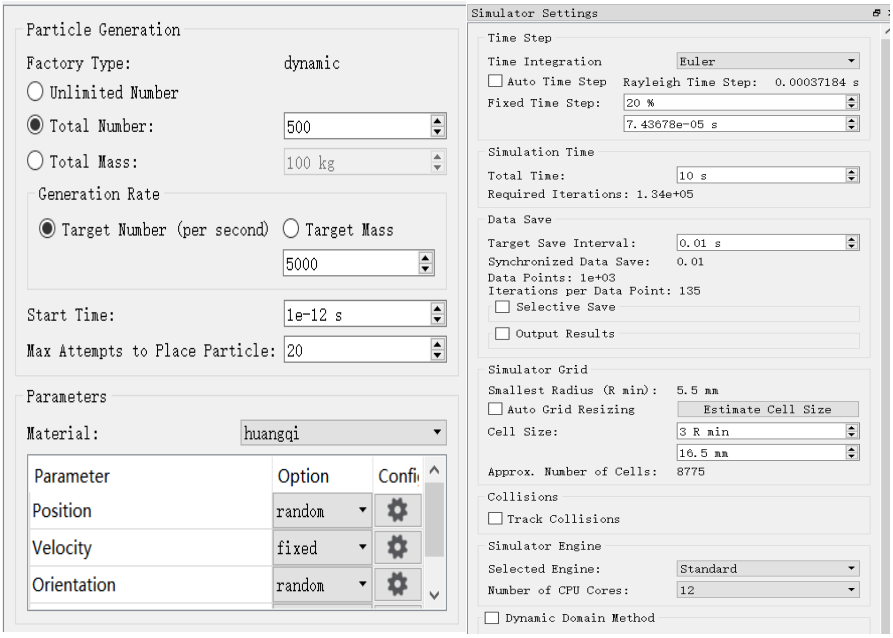

Fig. 10 - EDEM working parameter setting diagram

The particle dynamic generation plant was established in the inner position of the carton, and 500 astragalus segments were modelled to be generated in one second, and the plate on one side of the carton was withdrawn at 4s, and the astragalus segments were free to pour down under gravity, and the astragalus segments were stationary on the substrate after a period of 6s to form an astragalus pile, as shown in Fig. 11.

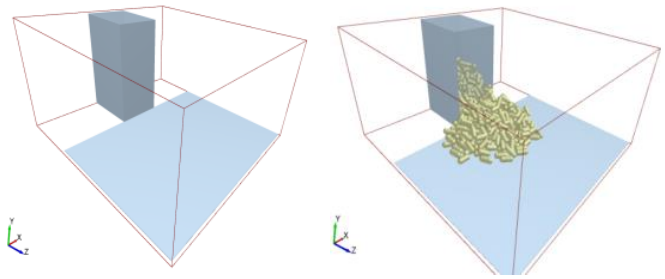

Fig. 11 - Simulation test of angle of repose of astragalus

Discrete element simulation parameter calibration

Plackett-Burman test

The Plcakett-Burman test was designed using Design-Expert11 software, with the simulated resting angle of astragalus as the response value and the parameters measured in the physical test as the test parameters, and the maximum and minimum values of the measured results were coded as the +1 and -1 levels, and the parameters that had a significant effect on the resting angle of astragalus were derived from the results of the Plcakett-Burman test. The Plcakett-Burman test level coding table with test protocol and results are shown in Table 3 and Table 4.

Table 3

Test parameters table

NO.	Test parameters	Low level (-1)	High level (+1)
A	Poisson's ratio	0.22	0.28
B	Astragalus-Astragalus collision recovery coefficient	0.2	0.4
C	Astragalus-Astragalus static friction coefficient	0.62	0.68
D	Astragalus-Astragalus rolling friction coefficient	0.5	0.56
E	Astragalus-steel collision recovery coefficient	0.3	0.4
F	Astragalus-steel static friction coefficient	0.1	0.3
G	Astragalus-steel rolling friction coefficient	0.1	0.2

Table 4

Design and results of the Plackett-Burman experiment

No.	Test Parameters							Repose angle
	A	B	C	D	E	F	G	θ (°)
1	1	1	-1	1	1	1	-1	43.93°
2	-1	1	1	-1	1	1	1	43.27°
3	1	-1	1	1	-1	1	1	30.11°
4	-1	1	-1	1	1	-1	1	28.7°
5	-1	-1	1	-1	1	1	-1	36.13°
6	-1	-1	-1	1	-1	1	1	29.68°
7	1	-1	-1	-1	1	-1	1	22.78°
8	1	1	-1	-1	-1	1	-1	32.62°
9	1	1	1	-1	-1	-1	1	23.75°
10	-1	1	1	1	-1	-1	-1	22.78°
11	1	-1	1	1	1	-1	-1	21.31°
12	-1	-1	-1	-1	-1	-1	-1	20.8°

The results of the experiment were analysed by ANOVA using Design-Expert software, as shown in Table 5.

Table 5

The Plackett-Burman test parameter significance affects the results

Parameters	Degree of freedom	Sum of squares	F-value	P-value
A	4.04	1	0.5648	0.4941
B	97.13	1	13.59	0.0211
C	0.0936	1	0.0131	0.9144
D	0.7203	1	0.1008	0.7668
E	109.69	1	15.35	0.0173
F	475.27	1	66.49	0.0012
G	0.0560	1	0.0078	0.9339

Note: 0.01<P<0.05, significant effect; P<0.01, highly significant effect; P>0.05, no significant effect.

As can be seen from Table 5, by carrying out the Plackett-Burman test, the astragalus-astragalus collision recovery coefficient (B), astragalus-Steel collision recovery coefficient (E) and astragalus-Steel static friction coefficient (F) were screened as significant factors.

Steepest climb experimental design

On the basis of Plackett-Burman test, the steepest climb test was conducted for the significance factors, and the relative error between the rest angle of the physical test and the rest angle of the simulation test was used as the evaluation index to determine the range of optimal intervals for the significance factors (*Ma at al., 2020*), and the other parameters were averaged for the simulation test.

Table 6

Design and results of the steepest climbing test

No.	Test Parameters			Repose angle	Relative error (%)
	B	E	F	θ (°)	
1	0.2	0.3	0.1	40.73°	13.8%
2	0.24	0.32	0.14	39.91°	11.5%
3	0.28	0.34	0.18	37.48°	4.7%
4	0.32	0.36	0.22	35.47°	0.89%
5	0.36	0.38	0.26	37.9°	5.9%
6	0.4	0.4	0.3	40.3°	12.6%

The design scheme and results of the steepest climb test are shown in Table 6. The Box-Behnken response surface design was carried out with level 4 as the centre point in the steepest climb test, and levels 3 and 5 as the low and high levels, respectively.

All other parameters in the simulation tests were averaged using physical test measurements: the Poisson's ratio of astragalus was taken to be 0.25, the coefficient of static friction between astragalus and astragalus was taken to be 0.65, the coefficient of rolling friction between astragalus and astragalus was taken to be 0.53, and the coefficient of rolling friction between astragalus and steel was taken to be 0.15 (*Hou et al., 2021*).

Box-Behnken experimental design

The Box-Behnken simulation test with significant contact parameters was designed using Design Expert11 software to calibrate the astragalus simulation parameters. The level 4 in the steepest climb test was taken as the centre point (0), and levels 3 and 5 were taken as the low level (-1) and high level (1), respectively, and the level coding table is shown in Table 7, and the Box-Behnken test design scheme and results are shown in Table 8.

Table 7

Significant exposure parameter level coding table

Levels	Astragalus -Astragalus Collision coefficient of restitution	Astragalus -Steel plate Collision coefficient of restitution	Astragalus -Steel plate static friction coefficient
-1	0.28	0.34	0.18
0	0.32	0.36	0.22
+1	0.36	0.38	0.26

Table 8

Box-Behnken experimental design and results of significant contact parameters

No.	Astragalus -Astragalus Collision coefficient of restitution	Astragalus -Steel plate Collision coefficient of restitution	Astragalus -Steel plate static friction coefficient	Repose angle θ (°)
1	-1	-1	0	40.69°
2	1	-1	0	34.67°
3	-1	1	0	34.51°
4	1	1	0	38.3°
5	-1	0	-1	34.99°
6	1	0	-1	34.78°
7	-1	0	1	36.75°
8	1	0	1	34.57°
9	0	-1	-1	37.23°
10	0	1	-1	33.04°
11	0	-1	1	34.51°
12	0	1	1	35.97°
13	0	0	0	36.13°
14	0	0	0	35.72°
15	0	0	0	35.75°
16	0	0	0	34.72°
17	0	0	0	35.91°

Multiple regression analysis of the experimental results in the table was carried out using Design-Expert11 software to obtain a second-order regression model for the simulated resting angle of astragalus with three significance parameters with the equation:

$$\begin{aligned}\theta = 35.65 - 0.5775\times A - 0.66\times B + 0.22\times C \\ + 2.45\times AB - 0.4925\times AC + 1.41\times BC \\ + 0.7408\times A^2 + 0.6557\times B^2 - 1.11\times C^2\end{aligned} \quad (5)$$

The p-value of the fitted model is less than 0.01, the coefficient of determination R^2 is 0.9717, the corrected coefficient of determination R^2adj is 0.9354, both close to 1, and the signal-to-noise ratio (Adeq precision) is 22.7736, which indicates that the angle of repose regression model is highly significant and predicts the target angle of repose; and the coefficient of variation, C.V. = 1.25%, is low, which indicates that the equations are well fitted . As shown in Table 9, it is indicated that the regression model is extremely significant, can reliably and realistically reflect the real situation, and can be used for further analysis of target angle of repose prediction.

Table 9

Analysis results of Box-Behnken test

Source of variation	Mean Square	Degree of freedom	Sum of Squares	P-value
Model	5.38	9	48.45	0.0001
B	2.67	1	2.67	0.0083
E	3.48	1	3.48	0.0042
F	0.3872	1	0.3872	0.2081
BE	24.06	1	24.06	<0.0001
BF	0.9702	1	0.9702	0.0642
EF	7.98	1	7.98	0.0004
B^2	2.31	1	2.31	0.0116
E^2	1.81	1	1.81	0.0200
F^2	5.23	1	5.23	0.0014
Residual	0.2013	7	1.41	
Lack of Fit	0.0772	3	0.2317	0.8498
Pure Error	0.2944	4	1.18	
Sum		16		

Note: 0.01<P<0.05, significant effect; P<0.01, highly significant effect; P>0.05, no significant effect.

Simulation parameter calibration and experimental verification

In the optimization module of Design-Expert11 software, the second-order regression equation (Eq. 5) was optimized and solved using the angle of repose of 35.79° measured in the physical tests as the target value, and a set of parameters similar to the data of the physical tests was obtained: the collision recovery coefficient of astragalus-astragalus was 0.32, the collision recovery coefficient of astragalus-Steel was 0.36, and the coefficient of static friction of astragalus-Steel was 0.22 The values of the remaining non-significant parameters were taken as the average of the physical test measurements.

Fig. 12 - Test comparison of repose angle of astragalus membranaceus

To check whether the optimal parameter combinations could meet the simulation test results, the above parameters were input into EDEM2018 software to carry out the validation test, and the validation test was repeated three times, and the resulting angles of repose of astragalus were 35.51°, 36.01°, and 35.43°, with an average value of 35.65°. The relative error between the simulation test result of angle of repose under the optimal parameter combination (35.65°) and the angle of repose measured in the physical test (35.79°) was 0.392%, which verified the reliability and authenticity of the simulation test. The test comparison is shown in Figure12.

The basic physical property parameters and contact parameters of astragalus were measured by physical tests, and the average values of collision recovery coefficient, static friction coefficient and rolling friction coefficient between astragalus were obtained as 0.3±0.1, 0.65±0.03, 0.53±0.03, respectively; and the average values of collision recovery coefficient, static friction coefficient and rolling friction coefficient between astragalus and steel were obtained as 0.35±0.05, respectively, 0.2±0.1, 0.15±0.05. The Plackett-Burman test was carried out to screen astragalus-astragalus collision recovery coefficient, astragalus-steel collision recovery coefficient and astragalus-steel static friction coefficient as significant factors affecting the angle of repose of astragalus.

CONCLUSIONS

Based on the physical property parameters measured in physical experiments, simulation experiments were conducted to establish a second-order regression model for the relative error between the simulated and physical experiment angles of repose. The optimal simulation parameters for astragalus membranaceus were obtained: astragalus membranaceus- astragalus membranaceus collision recovery coefficient of 0.32, astragalus membranaceus-steel collision recovery coefficient and static friction coefficient of 0.36 and 0.22, respectively.

The relative error between the average angle of repose in the astragalus membranaceus simulation experiment and the average angle of repose in the physical experiment is 0.392%, which further verifies the authenticity and feasibility of the simulation experiment and calibrated simulation parameters, providing a basis for subsequent research.

ACKNOWLEDGEMENT

This work was funded by the Key R&D and achievement transformation plan project of Inner Mongolia (2023YFDZ0006), the Program for improving the Scientific Research Ability of Youth Teachers of Inner Mongolia Agricultural University (BR220128), the Research Program of science and technology at Universities of Inner Mongolia Autonomous Region (NJZZ23046), and the High-level Talent Introduction and Research Launch Project of Inner Mongolia Agricultural University (NMGIRT2403).

REFERENCES

[1] Chen, L., Chen, Z., Hou, Z., et al. (2018). Experimental study of pilling coating parameters of forage seeds based on vibration action. *Research on agricultural mechanization*, 40(10):189-193. China.

[2] Cui, Z. (2014). Uses of Astragalus and the application of its cultivation and planting techniques. *Heilongjiang Pharmaceuticals*, 27(04):821-825. China.

[3] Dai, N., Hou, Z., Qiu, Y., et al. (2021). Calibration and testing of discrete meta-simulation parameters for red clover seeds. *Journal of Hebei Agricultural University*, 44(06):92-98. China.

[4] Hou, Z., Chen, L., Chen, Z., et al. (2021). Research on the movement law and parameter optimization of pelletized coating of forage seed. *Research on agricultural mechanization*, 43(11):184-191. China.

[5] Hou, Z., Dai, N., Chen, Z., et al. (2020). Determination of physical property parameters of iceplant seeds and calibration of parameters for discrete element simulation. *Journal of Agricultural Engineering*, 36(22):36-42. China.

[6] Huang, S., Shen, Y., Ou, C. (2023). Astragalus membranaceus and Panax notoginseng saponins improves intestinal L-arginine absorption and protects against intestinal disorder in vivo. *Food Science and Technology Research*, 29(2):129-140. China.

[7] Jiang, L., Zhang, D., Hao, X., et al. (2013). Overview of Astragalus development in Inner Mongolia. *Disease Surveillance and Control*, 7(03):165-166. China.

[8] Kang, Q., Yuan, H., Hu, Y., et al. (2016). Benefits and Prospects of Herbal Medicine Astragalus in Heilongjiang Province. *Heilongjiang Agricultural Science*, 08:118-121.China.

[9] Li, F., Liu, F., Liu, S., et al. (2015). Discussion on the items and methods to be measured for ultrasonic cleaning of traditional Chinese medicine Astragalus membranaceus. *Journal of Animal Husbandry and Veterinary Medicine*, 34(05):45-49. China.

[10] Liu, M., Hou, Z., Ma, X., et al. (2022). Discrete element-based simulation parameter calibration and testing of alfalfa seeds. *Jiangsu Agricultural Science*, 50(06):168-175. China.

[11] Ma, Y., Song, C., Xuan, C., et al. (2020). Parameter calibration of discrete element model for alfalfa straw compression simulation. *Journal of Agricultural Engineering*, 36(11):22-30. China.

[12] Shen M., Wang Y., Liu Z., et al. (2023). Inhibitory Effect of Astragalus Polysaccharide on Premetastatic Niche of Lung Cancer through the S1PR1-STAT3 Signalling Pathway. *Evidence-Based Complementary and Alternative Medicine*, 2023, 1-10. China.

[13] Wang, Y., Liang, Z., Zhang, D., et al. (2016). Discrete element-based calibration of interspecies contact parameters for corn seed particle models. *Journal of Agricultural Engineering*, 32(22):36-42. China.

[14] Wu, F., Chen, X., et al. (2004). A review on the pharmacological effects of Astragalus membranaceus. *Chinese herbal medicine*, 03:232-234. China.

[15] Zhang, L., Guo, B., Zhu, S., et al. (2006). Survey Report on Astragalus Germplasm Resources. *Chinese herbal medicine*, 2006(08):771-773. China.

[16] Zhang, T., Liu, F., Zhao, M., et al. (2018). Determination of physical parameters of corn stover contact and calibration by discrete element simulation. *Journal of China Agricultural University*, 23(4):120-127. China.

[17] Zhao, S. (2017). Prospect analysis and large-scale mechanized planting technology of astragalus. *Special economic flora and fauna*, 20(04):25-27. China.